MethodsX 10 (2023) 102224

Contents lists available at ScienceDirect

MethodsX

journal homepage: www.elsevier.com/locate/mex

Simple multi-residue analysis of persistent organic pollutants and molecular tracers in atmospheric samples ☆

Minas Iakovides [a,*], Jean Sciare [a], Nikos Mihalopoulos [a,b,c]

[a] Climate and Atmosphere Research Center (CARE-C), The Cyprus Institute, 20 Konstantinou Kavafi Str., Aglantzia 2121, Cyprus
[b] Chemistry Department, University of Crete, Heraklion Crete 71003, Greece
[c] Institute for Environmental Research and Sustainable Development, National Observatory of Athens, Palaia Penteli, Athens 15236, Greece

ARTICLE INFO

Method name:
Simple multi-residue analysis of persistent organic pollutants and molecular tracers in atmospheric samples.

Keywords:
PCBs
OCPs
PAHs
Hopanes
Steranes
Negative chemical ionization
GC/MS
Optimization

ABSTRACT

We present a simple, selective and sensitive analytical method to quantitatively determine a wide range of halogenated persistent organic pollutants and molecular tracers in atmospheric samples. Identification and quantification was carried out by high-resolution gas chromatography, hyphenated with low-resolution mass spectrometry operating in electron impact (EI) and electron capture negative ionization (ECNI) mode. Optimization on a number of instrumental parameters was conducted to obtain ultra-trace detection limits, in the range of few fg/m^3 for organohalogen compounds. Repeatability and reproducibility of the method was thoroughly evaluated. The analysis was validated with standard reference materials and successfully applied to actual atmospheric samples. The proposed multi-residue method provides a precise, affordable and practical procedure of sample analysis for environmental research laboratories with conventional instrumentation on a routine basis.

- A simple combination of alumina, florisil and silica gel adsorbents was applied to sufficiently isolate polychlorinated biphenyls, organochlorine pesticides, polycyclic aromatic hydrocarbons, long chain *n*-alkanes, hopanes and steranes.
- Full elution was achieved in two successive fractions, using small volumes of *n*-hexane and *n*-hexane/dichloromethane to recover all target substances.
- To maximize analytical response, optimization was applied for three operating parameters in ECNI mode: i) ion source temperature; ii) emission current; and iii) electron energy.

Specifications table

Subject area:	Environmental Science
More specific subject area:	Analytical method
Name of your method:	Simple multi-residue analysis of persistent organic pollutants and molecular tracers in atmospheric samples.
Name and reference of original method:	EPA Method 3610B, Alumina Cleanup (1996, December), SW-846 Ch 4.2.2 EPA Method 3620C, Florisil Cleanup, (2014, July), SW-846 Update V EPA Method 3630C, Silica Gel Cleanup, (1996, December), SW-846 Ch 4.2.2
Resource availability:	N. A.

☆ Related research articles US EPA method 3610B; US EPA method 3620C, US EPA method 3630C

* Corresponding author.
E-mail address: m.iakovides@cyi.ac.cy (M. Iakovides).

https://doi.org/10.1016/j.mex.2023.102224
Available online 17 May 2023

Method details

Introduction

Over the past decades, research on persistent organic pollutants (POPs), such as polychlorinated biphenyls (PCBs) and organochlorine pesticides (OCPs), has received growing attention within the scientific community. POPs are characterized by their acute toxicity in humans and biota [1,2], resistance to biological and photochemical degradation [3,4] and the ability to undergo long-range atmospheric transport (LRAT) far from emission sources [5]. Despite prohibition, which dates back to early 1980′s [6], illicit production and/or usage of industrial and pesticide grade POPs is still documented at a global scale [7–10]. Similarly to POPs, polycyclic aromatic hydrocarbons (PAHs) comprise a cluster of carcinogenic and mutagenic compounds of significant environmental concern [11–13], characterized by susceptibility to LRAT [14] and widespread distribution in the environment [15]. PAHs, usually formed during incomplete combustion of organic materials (e.g. fossil fuels, wood, coal) [16], have been widely used, along with long-chain *n*-alkanes, pentacyclic triterpanes and sterols, as molecular tracers of combustion sources and petroleum utilization [14,17,18].

The atmosphere acts as reservoir for a wide spectrum of organic compounds of different physico-chemical properties, receiving strong contributions from terrestrial and marine environments [19,20]. Semi-volatile organic compounds (SVOCs), such as those mentioned above, are usually present in both phases (gas and particulate) [21], while their distribution depends on vapor pressure, which governs the partitioning, and is strongly influenced by ambient temperature and aerosol properties [22]. Among all types of environmental matrices (sediment, soil, water, sewage sludge, fly ash), atmospheric samples are still challenging in treatment and chemical analysis [23,24], given the multitude and complexity of their organic content [25] typically present at trace amounts. It is therefore of particular importance the selection of a proper analytical technique, which ensures suitability in identification and quantification of SVOCs. Site location [26], sampling type and duration [27], in addition to sample volume, are also critical parameters in method selection and deployment.

To date, a plethora of studies aiming to propose novel analytical techniques, or modifications to already established ones, for the determination of SVOCs, particularly POPs and PAHs, can be found in the literature [comprehensive reviews from Maceira et al. [28]; Muscalu and Górecki [29]; Pico et al. [30]; Sathishkumar et al. [31] and references therein]. Additionally, to address potential challenges encountered from the analysis of complex mixtures in diverse sample matrices, several reference methods for sample extraction and clean-up processes (e.g. methods 3610B, 3620C and 3630C among others) were introduced by the US Environmental Protection Agency (USEPA) and other relevant authorities. These reports usually focus on individual or combined features of analysis, such as sample extraction, separation from interfering co-extractables and instrumental analysis, furnishing the scientific community with essential information towards selectivity and sensitivity, time effectiveness and/or cost efficiency. Although each of the aforementioned facets in method selection is equally crucial [32], combination is rather challenging and requires either modern instrumentation, or laborious sample preparation [30].

Gas chromatography (GC) hyphenated with high-resolution (HR) triple quadrupole (QqQ), time-of-flight (TOF), Orbitrap and Fourier-transform ion cyclotron resonance (FT-ICR) mass spectrometry (MS), even multi-dimensional gas chromatography coupled with HR-MS [28,29] were proven to substantially increase sensitivity and selectivity; however, a major issue is their high capital and operational costs. Particularly during periods where features of energy crisis are becoming more complicated and financial uncertainty affects research infrastructure [33,34], efforts by analysts move towards refining methods of analysis, which practically combine enhanced purification with the highest possible sensitivity using conventional low-resolution MS (LRMS) instrumentation.

On account of the above, we developed a precise and simple multi-residue analytical method, whose steps expand from sample purification to optimization on several mass spectrometric ionization parameters, for the quantitative determination of a large panel of POPs, PAHs and other selected molecular tracers in atmospheric samples. Fractionation was achieved by flash chromatography using small amounts of adsorbents and elution solvents, resulting in adequate recoveries. Optimization was carried out to maximize sensitivity on chemical analysis of target organohalogens. The proposed method was validated through a rigorous quality assurance/quality control procedure, and successfully applied to both gaseous and particulate phase atmospheric samples, collected at an urban location in the eastern Mediterranean.

Experimental

Materials and reagents

All standard mixtures used for method validation and instrumental response were prepared from high purity native and perdeuterated standard solutions. The corresponding part numbers for each commercial mixture are listed in Table S1 (Supporting Information (SI)). In particular, the long-chain *n*-alkanes (*n*-C_x) mixture [from *n*-undecane (*n*-C_{11}) to *n*-pentatriacontane (*n*-C_{35})], the parent PAHs mixture [naphthalene (Na), acenaphthylene (Acena), acenaphthene (Ace), fluorene (Flu), phenanthrene (Phe), anthracene (An), fluoranthene (Fluo), pyrene (Py), benzo[*a*]anthracene (B[*a*]A), chrysene/triphenylene (Chr/T), benzo[*b/j*]fluoranthene (B[*b*]F), benzo[*k*]fluoranthene (B[*k*]F), benzo[*a*]pyrene (B[*a*]P), dibenzo[*a,h*]anthracene (DB[*ah*]A), benzo[*g,h,i*]perylene (B[*ghi*]P), indeno[1,2,3-*c,d*]pyrene (IP)], phenanthrene-D_{10}, anthracene-D_{10}, pyrene-D_{10}, perylene-D_{12}, PCBs #54, 155, 185 and 204 (IUPAC nomenclature), the pesticide mixture [aldrin (ALDR), *cis*-chlordane (c-CHL), *trans*-chlordane (t-CHL), *oxy*chlordane (oxyCHL), chlorothalonil (CHLTHL), *o,p'*-DDD, *p,p'*-DDD, *o,p'*-DDE, *p,p'*-DDE, *o,p'*-DDT, *p,p'*-DDT, dicofol (DICF), dieldrin (DIELD), α-endosulfan (α-ENDS), β-endosulfan (β-ENDS), endosulfan sulfate (ENDSLF), endrin (ENDR), α-, β-, γ- and δ-hexachlorocyclohexane (HCH), heptachlor (HEPT), heptachlor exo-epoxide (*cis*-, isomer B) (HEPTEP), hexachlorobenzene (HCB)], α-HCH-D_6, *p,p'*-DDE-D_8, *p,p'*-DDT-D_8

and β-endosulfan-D_4 were all purchased from LGC (Germany). The PCB mixture [IUPAC nomenclature: PCB#17, 18, 28, 31, 33, 44, 49, 52, 70, 74, 82, 87, 95, 99, 101, 105, 110, 118, 128, 132, 138, 149, 151, 153, 156, 158, 169, 170, 171, 177, 180, 183, 187, 191, 194, 195, 201, 205, 206, 208, 209] was purchased from Accustandard (USA). Pristane, phytane, *n*-hexadecane-D_{34} and *n*-tetracosane-D_{50} were purchased from Neochema (Germany). 17α(H),21β(H)-hopane (C30$\alpha\beta$), 17α(H)−22,29,30-trisnorhopane (*Tm*), 5α,14α,17α-cholestane(20R) (C27$\alpha\alpha\alpha$R) and 5α,14α,17α-cholestane(20R)-D_6 (C27$\alpha\alpha\alpha$R-D_6) were purchased from Chiron (Norway). NIST's (National Institute of Standards and Technology) Standard Reference Material (SRM) 1649b (urban dust) was purchased from LGC (Germany). Glass wool, used for column packing, was purchased from Merck.

All solvents (*n*-hexane, dichloromethane, acetone, water) were of organic trace analysis grade (Unisolv/Suprasolv MS) and purchased from Merck (Germany). Florisil (magnesium silicate, 60–100 mesh) was of PR grade and purchased from Supelco (USA). Silica gel (silicon dioxide, 70–230 mesh), neutral alumina (aluminum oxide, 70–230 mesh) and anhydrous sodium sulfate (Na_2SO_4) were all of >99% purity and purchased from Merck. Glass microfiber (GF/A) filters (140 mm diameter) and polyurethane foam (PUF) plugs (100 × 140 mm) were purchased from Whatman (UK) and Klaus Ziemer (Germany), respectively.

Preceding sampling, GF/A filters were wrapped in Al foil and baked at 420 °C for 3 h. PUFs were thoroughly washed with soap, rinsed with fresh tap water, boiled for 5 h in nanopure water and then Soxhlet-extracted (ca. 3 cycles/h), first with acetone and then with *n*-hexane:dichloromethane (1:1) for a total of 48 h. After extraction, PUFs were placed in clean vacuum desiccators, dried for 72 h and wrapped with Al foil, placed into sealed zip-lock bags and stored at −18 °C until use. A custom-made borosilicate glass flash column (180 mm length × 0.5 mm OD, with capillary ending) was used for sample clean-up and separation process. At the top, the column was quick-fit joined with a glass solvent flow adapter and controller, whereas a Teflon stopcock was fitted at the bottom. Nitrogen gas (99.999% purity) was used for column packing and flow control. A custom-made cooling bath was used during evaporation under nitrogen pressure to preserve the process at temperatures below −5 °C. All laboratory glassware was thoroughly soap-washed with a phosphate-free detergent and rinsed first with tap water, and then with nanopure water (18.2 MΩ), acetone and *n*-hexane.

Air sampling

A total number of six atmospheric (gaseous and particulate phase) samples were separately collected for 24 h (08:00–08:00 UTC), using a high-volume (ca. 0.6 m^3/min) Digitel air sampler (DH77, Switzerland) equipped with a PM_{10} head, following by an adsorbent cartridge. The sampler was located at the rooftop of a three-story building in the facilities of the Cyprus Institute (Nicosia, Cyprus). GF/A filters and PUF plugs were used for the collection of particulate and gaseous phase samples. More details about the sampling site can be found in Iakovides et al. [8]. After sampling, all gaseous and particulate filters were wrapped in Al foil, sealed in zip-lock bags and stored at −18 °C until analysis.

Sample extraction

Samples were separately extracted in a Soxhlet apparatus, using a mixture of *n*-hexane:dichloromethane (1:1) for 24 h (ca. 3 cycles/h). Preceding extraction, all samples were spiked with given amounts of surrogate standards (GF/A filters: 20 ng of phenanthrene-D_{10}, pyrene-D_{10}, perylene-D_{12} for PAH analysis; 3 ng of PCBs #54, 155 and 185, and 8 ng of *p,p′*-DDE-D_8, *p,p′*-DDT-D_8, α-HCH–D_6 and β-endosulfan-D_4 for the analysis of organochlorines; PUF plugs: 100 ng of phenanthrene-D_{10}, pyrene-D_{10}, perylene-D_{12} for PAH analysis; 9 ng of PCBs #54, 155, 185 and 24 ng of *p,p′*-DDE-D_8, *p,p′*-DDT-D_8, α-HCH-D_6 and β-endosulfan-D_4 for the analysis of organochlorines), which correspond to the respective amounts in the atmosphere [35,8]. After extraction, each sample was transferred to a flask, solvent-exchanged to *n*-hexane and concentrated to ca. 2 ml using a vacuum rotavapor (Rotavap RV 300; Büchi, Switzerland) and a gentle stream of nitrogen.

Flash column preparation

Sodium sulfate and glass wool were separately extracted with *n*-hexane:dichloromethane (1:1) in a Soxhlet apparatus (ca. 3 cycles/h) for 24 h and dried into vacuum desiccators for at least 48 h, whereas given amounts were also baked at 420 °C for 3 h to ensure removal of trace contaminants, and stored into sealed glass jars. Alumina was activated at 300 °C for 16 h, whereas activation of silica gel and florisil was achieved at 200 °C for 12 h. It is worth noting that adsorbents should be activated upon the initiation of the clean-up procedure, while in advance activation should be avoided; all adsorbents used herein are hygroscopic and potential exposure to moisture air may alter their separation capability [36]. The adsorption column was filled from bottom to top with glass wool, 0.5 g of anhydrous Na_2SO_4, 1.0 g of activated silica gel, 1.0 g of activated alumina, 0.5 g of activated florisil and 1.0 g of anhydrous Na_2SO_4. Prior to sample loading, the adsorption column was properly packed under nitrogen pressure with a conditioning volume of ca. 20 ml *n*-hexane, while a constant flow rate of 1.0 ± 0.1 ml/min was also adjusted using a volumetric tube.

Instrumentation and chemical analysis

Chemical analysis of all target substances was carried out on an Agilent 7890B gas chromatograph, equipped with a cool on-column inlet operating at 3 °C above the corresponding temperature of the oven gradient (see below), and 9 ml/min septum purge flow. The GC was coupled with an Agilent mass selective detector (MSD inert 5977B), operating in electron impact (EI, 70 eV) and electron capture negative-ion chemical ionization (ECNI) mode. Methane (99.999% purity) was used as reagent gas in ECNI mode (2.0 ml/min

optimum flow rate). Transfer line was kept at 300 ˚C, while the MS quadrupole was modified at 150 ˚C. Ion source temperature in EI mode was set to 230 ˚C. Chromatographic separation was achieved on a 60 m × 0.25 mm ID × 0.25 μm film thickness and a 30 m × 0.25 mm ID × 0.25 μm film thickness non-polar 5%-phenyl-methylpolysiloxane columns (ultra-inert DB-5 ms; J&W, USA), for organochlorines and PAHs-aliphatics analysis, respectively. Capillary columns were coupled with a 3 m deactivated fused silica guard column (Agilent, USA) using ultra-inert press fits. Helium (99.999% purity) was used as carrier gas, with a constant flow rate of 1.0 ml/min. The GC oven gradients were optimized as follows: i) 50 ˚C initial temperature (held for 1 min), ramp to 150 ˚C at 30 ˚C/min, and then to 300 ˚C at 5 ˚C/min (held for 40 min) for PAHs (74.33 min total runtime); ii) 50 ˚C initial temperature (held for 1 min) and ramp to 300 ˚C at 5 ˚C/min (held for 20 min) for aliphatics (71 min total runtime); and iii) 50 ˚C initial temperature (held for 1 min), ramp to 140 ˚C at 30 ˚C/min, then to 285 ˚C at 2.2 ˚C/min and finally to 300 ˚C at 15 ˚C/min (held for 15 min) for organochlorines (85.91 min total runtime). All solutions were injected (2 μl volume) to GC–MS through a cool on-column injector, using an Agilent G4567A automated liquid sampler (ALS). PAHs and aliphatics were quantified based on relative response factor (RRF) calculations for each single organic substance (solutions of 0.2–19.5 and 1.5–3.9 ng/μl, respectively) in EI mode [8,37,38], whereas quantification of PCBs and OCPs was performed by external calibrations (sets of seven-level standard mixtures of 2, 10, 24, 43, 65, 105 and 250 pg/μl for PCBs, and 5, 23, 85, 169, 251, 389 and 647 pg/μl for OCPs) in ECNI mode. A maximum number of five samples per batch of GC–MS analysis were run, while in the event where RRFs and R^2 coefficients during calibration exhibited CV>20% and values <0.96, respectively, the analysis was discarded and went over again. Identification of each target compound was based on retention time (± 2 s) (Tables S2-S4, SI) and mass fractionation (± 15%) of reference standard mixtures run in scan mode (50–550 and 30–550 amu in EI and ECNI mode, respectively) [37]. Target and qualification ions, along with their mass fragments, are also presented in Tables S2-S4 (SI).

Results and discussion

Quality assurance/quality control of chemical analysis

Three sets of pre-cleaned PUF and GF/A field and procedural blanks were analyzed to calculate the corresponding blank amounts. All blanks received the same treatment applied to the exposed samples. Blank amounts were < 1.11% for *n*-alkanes (*n*-C_{11} - *n*-C_{15}), 0.64% for PAHs (phenanthrene to pyrene) and 0.02% for PCBs and OCPs (tri- and tetra-CBs). No detectable blank amounts were measured for pristane, phytane, C27$\alpha\alpha\alpha$R, *Tm* and C30$\alpha\beta$. Standard mixtures with concentrations spanning from 0.2 to 0.8, 0.07–0.3, 0.01–1.2 and 0.2–16.8 pg/μl for PAHs, aliphatics, PCBs and OCPs, respectively, were prepared and injected to GC–MS to calculate the detection limits of the instrument (IDL). The amounts of analytes that correspond to chromatographic peaks with a signal-to-noise (S/N) ratio over 3:1 were considered as detectable [39]. The detection limits of the method (MDL) were correspondingly calculated as their average amounts in blanks plus three times 1σ [39]. For analytes not detected in blanks, MDLs were estimated based on IDLs (Table 1), the average recovery of the analytical method (more details in section 3.2; see also Fig. 1), the average volume of air samples (650 m^3) and the final volume in the GC vial (20 μl) [37]. The estimated MDLs for the blank non-detectable analytes were experimentally evaluated by re-analyzing native standard mixtures in GC–MS at the predicted concentrations, and all exhibited S/N ratios > 6.3. MDLs for all target compounds are listed in Table 1.

Evaluation of adsorption column separation

To evaluate the performance of the column, the recovery of all target compounds throughout separation was checked using a standard mixture in varying amounts (ca. 600 ng for *n*-alkanes, 40–100 ng for pentacyclic triterpanes, 60–1200 ng for PAHs, 40–300 ng for PCBs and 40–70 ng for OCPs) depending on the concentration of the standard mixtures. The mixture (2 ml total volume) was prepared into a clean pear-shaped glass flask using gastight syringes. It was then inserted into the column and separation was achieved in two successive elusions: i) 14 ml of *n*-hexane; and ii) 30 ml of *n*-hexane:dichloromethane (1.7:1.3). The procedure was repeated in triplicate and all recoveries (± 1σ) are displayed in Fig. 1. In particular, PCB congeners (except for #169), *o,p'*-DDE, *p,p'*-DDE, heptachlor, HCB, aldrin and all aliphatics were collected with the first fraction (*n*-hexane; 14 ml), whereas all PAHs, PCB 169 and the remaining OCPs (namely *cis*-chlordane, *trans*-chlordane, oxychlordane, chlorothalonil, dieldrin, endrin, α- to δ-HCH, heptachlor epoxide, dicofol and the vast amounts of *o,p'*- and *p,p'*-DDD/Ts) were eluted in the second fraction (*n*-hexane:dichloromethane 1.7:1.3; 30 ml). Mass recoveries were satisfactory, exhibiting >90% on average for most *n*-alkanes (> *n*-C_{19}) and PCBs (> penta-CBs) in the first elution, whereas the less volatile *n*-alkanes (C_{11} to C_{17}), tri- and tetra-CBs showed relatively lower recoveries (ca. 80–85 and >80%, respectively), most likely due to evaporation losses [37]. Aldrin, heptachlor, HCB and DDEs were successfully recovered (>85%) during first elution with *n*-hexane, while low proportions (<15%) were collected in the second fraction. On the contrary, most PAHs (pyrene to benzo[*ghi*]perylene) and the remaining OCPs were almost fully recovered during second elution, exhibiting mass recoveries >90%, except for the low molecular weight PAHs (fluorene to anthracene), DDDs and at a lesser extent DDTs (Figs. 1B; 1D), which were partially eluted in the first fraction (<15%).

Total recoveries (summary of elution fractions 1 and 2) for most target compounds exhibited values >90%, except for some tri- & tetra-CBs (e.g. #18, 17, 33, 44, 70), as well as PCBs #99 and #110, which were recovered at relatively lower, yet acceptable, levels (78–86%). After a step-by-step examination of potential losses during i) rotary evaporation, and ii) final evaporation under nitrogen stream, most losses (up to 25%) occurred during rotary evaporation. Preservation of temperatures <−5 ˚C during evaporation under nitrogen stream showed recovery reduction at considerably lower levels (<10%), compared to the corresponding process under ambient laboratory temperatures, during which compound losses (up to 35%) sometimes exceeded those during rotary evaporation

Table 1
Instrumental (IDL) and method detection limits (MDL) for all target compounds.

Target compound	IDL [pg/μL]	MDL [fg/m^3]	Target compound	IDL [pg/μL]	MDL [fg/m^3]
#PCBs			PAHs		
#18	0.84	26.3	Fluorene	0.26	8.1
#33	0.79	24.8	Phenanthrene	0.27	8.5
#52	0.79	24.8	Anthracene	0.27	8.5
#70	0.52	16.3	Fluoranthene	0.54	17.1
#74	0.18	5.6	Pyrene	0.27	8.5
#82	0.09	2.7	Benzo[*a*]anthracene	0.27	8.5
#99	0.09	2.7	Chrysene/Triphenylene	0.27	8.5
#101	0.08	2.5	Benzo[*b/j*]fluoranthene	0.54	17.1
#118	0.09	2.7	Benzo[*k*]fluoranthene	0.27	8.5
#128	0.14	4.4	Benzo[*a*]pyrene	0.27	8.5
#149	0.48	14.9	Indeno[1,2,3-*c,d*]pyrene	0.27	8.5
#151	0.02	0.8	Dibenzo[*a,h*]anthracene	0.54	17.1
#169	0.07	2.1	Benzo[*g,h,i*]perylene	0.54	17.1
#180	0.08	2.5	OCPs		
#183	0.01	0.2	Aldrin	0.43	13.4
#187	0.03	0.9	*cis*-Chlordane	0.21	6.5
#195	0.01	0.4	*trans*-Chlordane	0.10	3.1
#205	0.01	0.2	oxychlordane	0.73	22.9
#209	0.01	0.2	Chlorothalonil	0.09	2.9
Aliphatics			*o,p´*-DDD	0.87	27.1
n-C_{11} – *n*-C_{17}	0.40	12.5	*p,p´*-DDD	1.70	53.1
n-C_{18} – *n*-C_{29}	0.35	10.9	*o,p´*-DDE	0.73	22.9
n-C_{30} – *n*-C_{31}	0.45	14.1	*p,p´*-DDE	2.80	87.5
n-C_{32} – *n*-C_{35}	0.65	20.3	*o,p´*-DDT	2.17	67.7
Pristane	0.50	15.6	*p,p´*-DDT	11.27	352.2
Phytane	0.50	15.6	Dicofol	2.80	87.5
C27$\alpha\alpha\alpha$R	1.10	34.4	Dieldrin	0.23	7.3
Tm	0.96	29.7	α-Endosulfan	0.13	4.0
C30$\alpha\beta$	0.90	28.1	β-Endosulfan	0.13	4.0
			Endosulfan sulfate	0.09	2.7
			Endrin	1.44	45.1
			α-HCH	0.73	22.9
			β-HCH	0.73	22.9
			γ-HCH	0.73	22.9
			δ-HCH	0.73	22.9
			Heptachlor	0.30	9.4
			Hexachlorobenzene	0.03	1.1
			Heptachlor exo-epoxide	0.83	26.0

(see above). Therefore, deployment of a cooling bath during last-step evaporation improves significantly the overall recovery of target compounds.

Optimization of MS conditions

Mass spectrometric operation parameters in ECNI mode were optimized to obtain high-mass fragment ion abundances and thus gain lower detection rates, compared to the corresponding parameterizations in EI and ECNI mode, which were based on the default tune settings using perfluorotributylamine (PFTBA) and perfluoro-5,8-dimethyl-3,6,9-trioxidodecane (PFDTD) as source calibrants. Ion source temperature, electron energy and emission current were selected to be optimized. Thermal aux and quadrupole temperature, ion source pressure and reagent gas flow rate were not investigated and kept unmodified at the default auto-tune adjustments, due to potential limited effects on analyte response (GC–MS interface and quadrupole temperature), peak tailing and matrix effects (source pressure, methane flow rate) [40–42]. A neat standard mixture of PCBs and OCPs at concentrations spanning from 0.5 to 0.7 ng/μl was prepared for the tests, whereas constant volumes of 2 μl were injected using the ALS. The optimized GC oven gradient (see section 2.5), interface and quadrupole temperatures (300 and 150 ˚C) and electron multiplier voltage (1187 V) were also held constant during optimization runs. Fragment ions and isotope peaks listed in Tables S3 and S4 (SI) for PCBs and OCPs were monitored, while all GC–MS runs were carried out in SIM mode. To the best of our knowledge, the current study is the first which reports optimum mass spectrometric conditions for PCBs and OCPs combined in a single run in ECNI mode.

High ion source temperatures yield in general considerable impacts on the formation and kinetics of the low-energy thermal electrons in the source chamber and influence the molecule-thermal electron interactions, leading to higher vibrational energies and thus stronger fragmentation of the molecular ions. Although ion source retains in principle temperatures from 0 to 300 ˚C, normally is adjusted between 150 and 250 ˚C [43,44], whereas at temperatures <150 ˚C the ion source acts as “cold-spot” for analytes passing through hot GC column and transfer line surfaces before entering the colder chamber, resulting in peak tailing

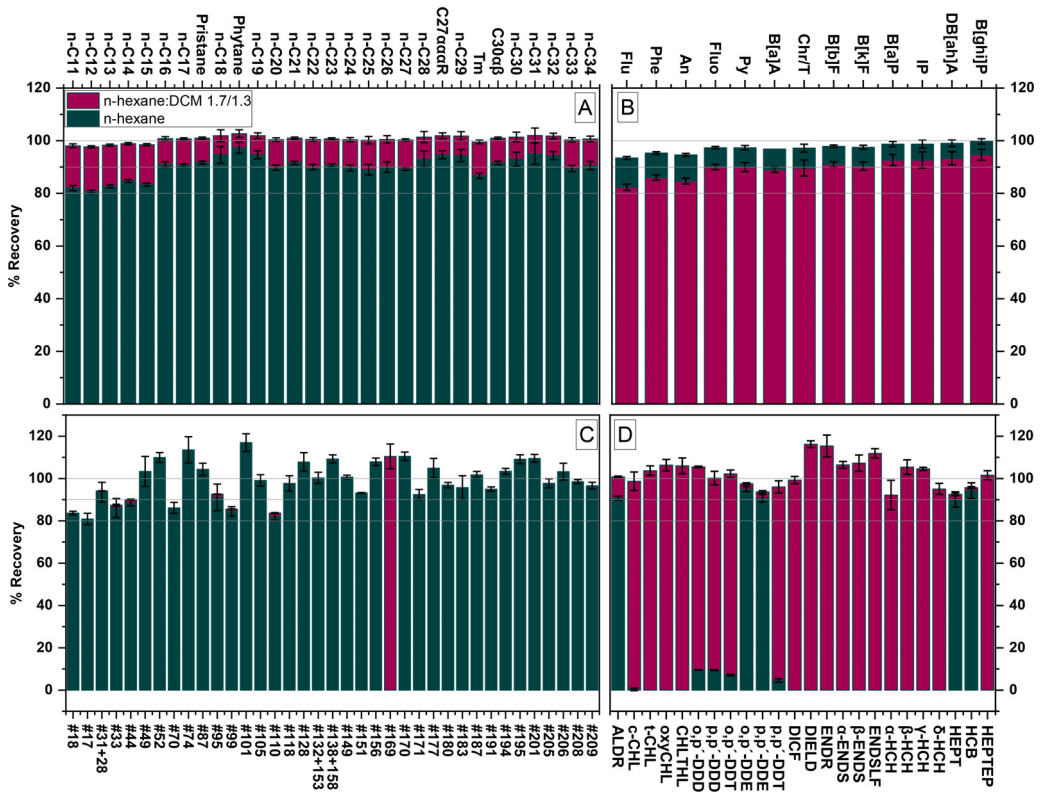

Fig. 1. Average (± 1σ) mass recoveries for all target compounds (A: aliphatics, B: PAHs, C: PCBs, D: OCPs) at the optimized clean-up procedure (n = 3).

and poor shaping. Nine ion source temperature intervals (140–250 ˚C) were investigated in our optimization tests (Fig. 2; panels A, D). High-mass fragment molecular ions of >hexa-CBs were most sensitive to source temperature, yielding decreased abundances as temperature increases, while chlorine ion abundances for tri- to penta-CBs showed insignificant (Kruskal-Wallis test, K-W; p>0.19) differences (<15%; Fig. 2A). Lower ion source temperatures yielded larger high-mass abundances for most OCPs, except for aldrin and oxychlordane, which both appeared with no significant (K-W; p>0.17) differences (<10%) in ion abundances as a function of temperature (Fig. 2D). Among OCPs, the highly electronegative heptachlor epoxide, HCB, heptachlor and HCHs exhibited the largest variability in molecular ion's responses (Fig. 2D). The observed tendency of larger peak abundances of molecular ions for analytes with higher chlorination when temperature in the source decreases, may be attributed to the higher thermal electron capture by compounds with higher electron affinity, particularly in the presence of methane in the chamber [45]. Similar behavior has also been reported for the brominated diphenyl ethers [40], with decreasing bromide ion abundances as a function of temperature, in contrast to the increasing high-mass fragment ion abundances. For most PCBs and OCPs, ion source temperature values of 140–150 ˚C yielded the largest peak abundances (Fig. 2A, D), however the optimal value of 150 ˚C was selected (Fig. 2A, D).

Ionization energies spanning from 50 to 225 eV were also manually inserted to inspect the corresponding response in peak signal (Fig. 2B, E). An increase in molecular ion abundances for >hexa-CBs (Fig. 2B) and OCPs (Fig. 2E) was observed as electron energy raises up, peaking at a value of 75 eV (optimal ionization energy). For penta-CBs, the increase in peak areas at 75 eV was measured shallower (ca. 20%) compared to more chlorinated ones, while tri- and tetra-CBs exhibited the least increase in peak areas (ca. 17% lower compared to penta-CBs). Similar behavior has been observed for aldrin and chlordane isomers, exhibiting a shallower, compared to other OCPs, peak increase at 75 eV, whereas sharper was the increase for heptachlor, HCB, HCHs and heptachlor epoxide (Fig. 2E). After peaking at 75 eV, ion abundances showed in general a decrease at an electron energy value of 100 eV, and then flattened at energies up to 225 eV (Fig. 2B, E).

Emission current was also optimized at eight different tune values (50, 75, 100, 125, 150, 175, 200 and 220 μA). A similar positive and linear trend was observed for both PCBs and OCPs, resulting in an optimal value of 220 μA (Fig. 2C, F). Relatively sharper increases in ion abundances were, as expected, displayed for analytes with higher electron affinity (>hexa-CBs and electronegative OCPs, such as heptachlor and its epoxide, HCB and HCHs). At this point, it is worth noting that setting an optimum emission current at its maximum (or close to its maximum) levels may result in filament deformation, or disarrangement over its location at the entrance hole of the source chamber, inducing shorter lifetimes and poor performance over time.

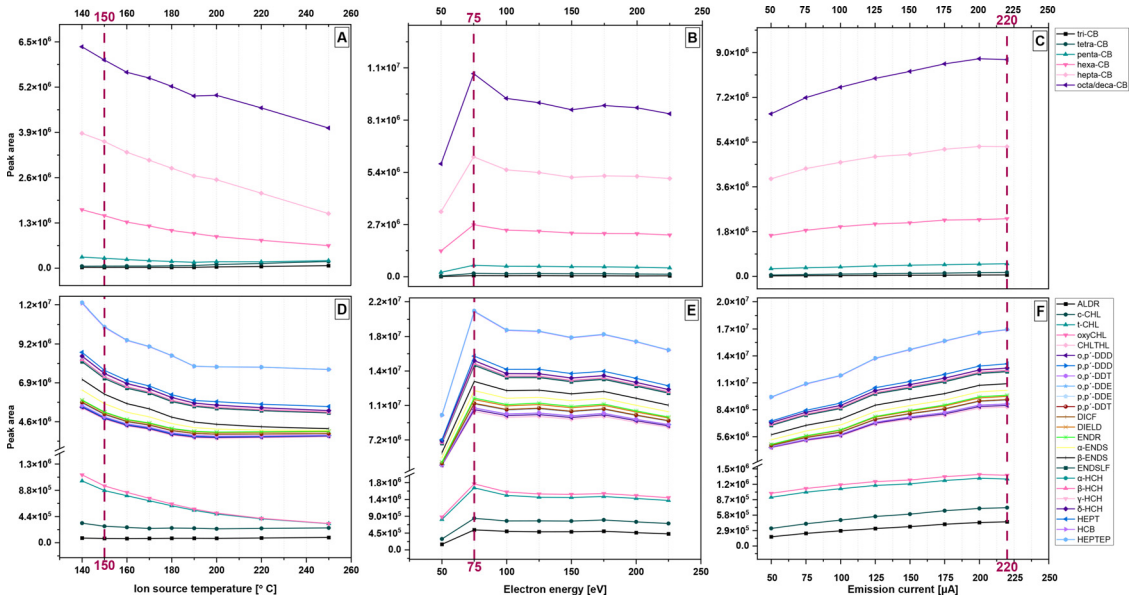

Fig. 2. Average peak areas of PCBs (panels A-C) and OCPs (panels D-F) yielded as a function of ion source temperature, electron energy and emission current. The resulted optimum values are highlighted with red.

Linearity of instrumental analysis

Once optimum mass spectrometric parameters were determined, the linearity of chemical analysis was evaluated by seven-point calibration curves, using native standard mixtures constructed within concentration ranges of 2–250 and 5–650 pg/μl for PCBs and OCPs, respectively, which reflect the approximate amounts in aerosol samples (see also section 2.5). Unlike native standard concentrations, the corresponding surrogate (120–130 and 395–410 pg/μl for PCBs and OCPs) and internal (110 and 370 pg/μl for PCBs and OCPs) standard concentrations were preserved at constant levels in all calibration mixtures. The resulting curves were blank offset and exhibited linear calibration coefficients (R^2) for PCBs ranging from 0.974 (tri- and tetra-CBs) to 0.999 (>hepta-CBs), and from 0.982 (*p,p'*-DDE and dicofol) to 0.998 (HEPT) for OCPs. Characteristic examples of calibration curves for PCBs #18, #183, *p,p'*-DDE and heptachlor are displayed in Fig. S1 (SI).

Repeatability and reproducibility of the method

Intra- and inter-assay precision of the analysis were both evaluated for all target substances on a two-way approach, and particularly by analyzing i) native standard mixtures at given concentrations; and ii) actual atmospheric samples. Six replicates of standard mixtures at concentrations of 1–5, 0.5–2, 0.03–0.12 and 0.2–0.3 ng/μl for aliphatics, PAHs, PCBs and OCPs, respectively, have been prepared and injected to GC–MS on the same day and under the same tune conditions. The analysis showed highly repeatable results, exhibiting coefficients of variation (CV) <11 and 9% for aliphatics and PAHs in EI mode, and <16 and 14% for PCBs and OCPs in ECNI mode. In addition to repeatability evaluations, the aforementioned standard mixtures were also run into GC–MS during specific time intervals (once per day for five consecutive days). The interday variance of the instrumental response (CV%) was satisfactory when applied to standard mixtures of predefined concentrations, with values <13 and 11% for aliphatics and PAHs, and <17 and 16% for PCBs and OCPs. Similar approaches were applied to evaluate repeatability and reproducibility of the proposed method in actual atmospheric samples. In particular, collected samples, already underwent the entire procedure of analysis (see also section 3.7), were randomly selected and analyzed in GC–MS i) for six times in one day; and ii) once per day for five successive days. The corresponding inter- and intraday variations (CV%) in atmospheric samples are presented in Tables 2 and 3. The methodology exhibited in general adequate inter- and intraday precisions (CVs up to 18 and 22%, respectively) when applied to atmospheric samples, highlighting the magnitude of robustness of the proposed method.

Performance of the method

To further validate the performance of the proposed analytical method throughout all of its steps (extraction, clean-up/fractionation and chemical analysis), the NIST's urban dust standard reference material (SRM 1649b) was used [46]. In particular, predefined amounts of SRM 1649b, reflecting the corresponding amounts of PM_{10} (1st quartile 21 $\mu g/m^3$) in the study environment [8], were obtained in triplicate (ca. 12 ± 1 mg each) and Soxhlet-extracted, preserving the same extraction conditions as with atmospheric samples (see section 2.3). The extracts were then concentrated, cleaned-up and analyzed following the procedure described above in detail.

Table 2
Average (± 1σ) concentrations of PAHs and aliphatic compounds in gas (n = 6) and particulate (n = 6) phase samples, intra- and inter-day variability (% CV) of selected samples.

PAH member	Gas phase	Particulate phase	Intra-day variability	Inter-day variability	Aliphatic compound	Gas phase	Particulate phase	Intra-day variability	Inter-day variability
	Average ± 1σ		CV			Average ± 1σ		CV	
	[ng/m^3]		[%]			[ng/m^3]		[%]	
Fluorene	2.43 ± 1.22	0.01 ± 0.004	13	15	n-C_{11}	0.18 ± 0.06	0.01 ± 0.004	11	16
Phenanthrene	11.08 ± 4.88	0.02 ± 0.01	9	12	n-C_{12}	0.25 ± 0.06	0.02 ± 0.004	12	18
Anthracene	0.94 ± 0.83	0.003 ± 0.002	11	14	n-C_{13}	0.22 ± 0.16	0.01 ± 0.01	14	14
Fluoranthene	2.72 ± 0.67	0.05 ± 0.02	9	12	n-C_{14}	0.38 ± 0.03	0.02 ± 0.002	12	15
Pyrene	2.75 ± 1.08	0.07 ± 0.02	8	13	n-C_{15}	0.41 ± 0.06	0.02 ± 0.002	14	12
Benzo[*a*]anthracene	0.02 ± 0.02	0.03 ± 0.02	12	16	n-C_{16}	1.42 ± 0.29	0.03 ± 0.01	13	14
Chrysene/Triphenylene	0.13 ± 0.07	0.11 ± 0.05	14	17	n-C_{17}	7.81 ± 1.82	0.15 ± 0.04	8	16
Benzo[*b/j*]fluoranthene	0.004 ± 0.002	0.13 ± 0.06	10	13	Pristane	9.81 ± 2.28	0.65 ± 0.15	11	17
Benzo[*k*]fluoranthene	0.002 ± 0.002	0.05 ± 0.03	9	14	n-C_{18}	3.85 ± 2.75	0.14 ± 0.12	6	14
Benzo[*a*]pyrene	0.001 ± 0.001	0.06 ± 0.03	9	11	Phytane	6.76 ± 4.82	0.17 ± 0.12	10	16
Indeno[1,2,3-*c,d*]pyrene	0.002 ± 0.001	0.08 ± 0.03	8	14	n-C_{19}	1.02 ± 0.75	0.08 ± 0.06	9	15
Dibenzo[*a,h*]anthracene	0.001 ± 0.001	0.01 ± 0.002	11	12	n-C_{20}	0.92 ± 0.24	0.11 ± 0.02	8	9
Benzo[*g,h,i*]perylene	0.004 ± 0.002	0.11 ± 0.04	10	11	n-C_{21}	0.50 ± 0.14	0.10 ± 0.03	9	11
ΣPAHs	20.08 ± 8.06	0.70 ± 0.27			n-C_{22}	0.66 ± 0.34	0.23 ± 0.12	11	13
					n-C_{23}	0.83 ± 0.57	0.46 ± 0.32	11	13
					n-C_{24}	0.53 ± 0.41	0.66 ± 0.51	13	15
					n-C_{25}	0.59 ± 0.37	0.96 ± 0.61	10	14
					n-C_{26}	0.21 ± 0.14	0.89 ± 0.61	8	15
					n-C_{27}	0.57 ± 0.32	1.12 ± 0.61	9	17
					n-C_{28}	0.12 ± 0.07	0.78 ± 0.48	6	18
					C27$\alpha\alpha\alpha$R	0.03 ± 0.01	0.02 ± 0.01	14	17
					n-C_{29}	0.77 ± 0.31	1.45 ± 0.57	11	16
					Tm	0.03 ± 0.01	0.03 ± 0.01	14	19
					C30$\alpha\beta$	0.13 ± 0.10	0.14 ± 0.11	13	18
					n-C_{30}	0.07 ± 0.04	0.68 ± 0.41	14	16
					n-C_{31}	0.34 ± 0.13	1.19 ± 0.44	15	17
					n-C_{32}	0.16 ± 0.11	0.37 ± 0.26	12	16
					n-C_{33}	0.11 ± 0.05	0.53 ± 0.27	14	17
					n-C_{34}	0.12 ± 0.08	0.23 ± 0.19	15	14
					n-C_{35}	0.06 ± 0.04	0.26 ± 0.19	13	18
					Σn-C_x	22.06 ± 4.42	10.48 ± 5.2		

The corresponding concentrations (average ± 1σ) for PAHs and aliphatics, as well as for PCBs and OCPs, are displayed in Figs. 3C and 3D (bar charts), respectively. SRM's certified and reference values (± uncertainties) on a dry-mass basis are also shown in the same panels for comparison. SRM's reference values for PAHs correspond to concentrations measured at different extraction conditions (Soxhlet or pressurized fluid extraction) and temperatures [46]. Zeta- (z-) and $\zeta\varepsilon\tau\alpha$- ($\zeta$-) scores for each SRM measurement were also calculated, based on the study of Analytical Methods Committee [47], and the corresponding scatterplots of $|$z-$|$ versus $|\zeta$-$|$ absolute scores for PAHs and PCBs-OCPs are displayed in Figs. 3A and 3B, respectively. Information values for a series of aliphatic compounds are also shown in Fig. 3C for comparison, however, these values lack of any assessed uncertainty information [46], and therefore were not included in z- and ζ-score calculations. Scores < 3 have been considered as acceptable and were both highlighted by light blue areas (Figs. 3A, 3B). D-scores (%) for all measured compounds were also calculated [47] and discussed below. The closer the D-score to zero, the closer the measured concentration is to the assigned value.

Certified values for PAHs (pyrene, chrysene/triphenylene, benzo[*b*]fluoranthene, benzo[*k*]fluoranthene and indeno[1,2,3 *cd*]pyrene) were adequately predicted, exhibiting a recovery range from 90 (pyrene) to 106% (chrysene/triphenylene) (Fig. 3C), and $|$D-score$|$ values from 6 (indeno[1,2,3 *cd*]pyrene) to 11 (chrysene/triphenylene) on average. The corresponding PAH reference values (fluorene, phenanthrene, anthracene, fluoranthene, benzo[*a*]anthracene, benzo[*a*]pyrene, dibenzo[*a,h*]anthracene and benzo[*g,h,i*]perylene) were measured at relatively lower, compared to those of certified values, recoveries and ranged from 87 (benzo[*g,h,i*]perylene) to 124% (fluorene) (Fig. 3C), with average $|$D-score$|$ values from 4 (phenanthrene) to 24 (fluorene). Similar observations have been obtained from the $|$z-$|$ against $|\zeta$-$|$ scores scatterplot for PAHs (Fig. 3A). In particular, less recovered PAH members (dibenzo[*a,h*]antracene and benzo[*g,h,i*]perylene) scored z- values higher than $|3|$ on average and among the highest ζ-values among PAHs (−1 and −2, respectively), yet lower than the respective threshold. Reference and certified PAHs with relatively lower associated uncertainties in SRM 1649b, such as anthracene (0.41 ± 0.004), benzo[*a*]anthracene (2.11 ± 0.05), chrysene (3.045 ± 0.028) and benzo[*k*]fluoranthene (1.702 ± 0.049) exhibited z- and/or ζ-scores higher than 3 in at least one out of three SRM measurements in total (Fig. 3A). Recovery ranges for n-alkanes spanned from 83 (n-C_{28}) to 141% (n-C_{22}) on average, whereas C27$\alpha\alpha\alpha$R and *Tm* were measured close to the respective mass fractions (average 95 and 93%) (Fig. 3A), with $|$D-scores$|$ among the lowest calculated for this particular compound group (average 6 and 7, respectively).

Certified mass fractions for the less chlorinated PCBs (# 49 and 52) were recovered at relatively lower levels (average 76 and 84%), compared to those of >penta-Cl biphenyls (> 91% on average for PCBs #105, 110, 149, 151, 183, 187, 194 and 206) (Fig. 3D).

Table 3
Average (± 1σ) concentrations of PCBs and OCPs in gas (n = 6) and particulate (n = 6) phase samples, intra- and inter-day variability (% CV) of selected samples.

PCB congener	Gas phase	Particulate phase	Intra-day variability	Inter-day variability	OCP compound	Gas phase	Particulate phase	Intra-day variability	Inter-day variability
	Average ± 1σ		CV			Average ± 1σ		CV	
	[pg/m^3]	[fg/m^3]	[%]			[pg/m^3]	[fg/m^3]	[%]	
#17	16.71 ± 0.85	69 ± 32	14	22	Aldrin	0.75 ± 0.32	28 ± 2	16	21
#18	7.44 ± 0.38	31 ± 2	12	20	*cis*-Chlordane	1.15 ± 0.34	23 ± 7	11	15
#31+28	25.96 ± 1.32	90 ± 37	15	17	*trans*-Chlordane	1.50 ± 0.34	37 ± 13	10	15
#33	6.01 ± 0.31	<MDL	11	18	*oxy*chlordane	0.41 ± 0.07	24 ± 8	11	16
#44	3.02 ± 0.15	42 ± 8	13	21	Chlorothalonil	11.64 ± 2.57	45 ± 8	10	13
#49	38.74 ± 1.98	243 ± 98	11	13	*o,p´*-DDD	0.22 ± 0.27	<MDL	17	21
#52	77.37 ± 3.94	214 ± 67	9	12	*p,p´*-DDD	2.93 ± 0.63	70 ± 11	13	16
#70	4.65 ± 0.24	78 ± 26	12	16	*o,p´*-DDE	9.35 ± 2.8	40 ± 6	15	17
#74	1.96 ± 0.1	29 ± 17	13	18	*p,p´*-DDE	2.01 ± 0.37	91 ± 3	11	14
#82	0.23 ± 0.01	13 ± 4	14	19	*o,p´*-DDT	24.01 ± 3.18	522 ± 90	10	15
#87	7.13 ± 0.36	9 ± 1	8	12	*p,p´*-DDT	38.79 ± 18.54	<MDL	13	17
#95	6.51 ± 0.33	18 ± 5	10	14	Dicofol	11.16 ± 1.15	128 ± 24	10	13
#99	0.95 ± 0.05	15 ± 8	13	17	Dieldrin	5.61 ± 9.85	114 ± 83	9	12
#101	6.91 ± 0.35	64 ± 18	10	13	α-Endosulfan	12.01 ± 4.02	187 ± 76	7	11
#105	0.11 ± 0.01	29 ± 23	11	15	β-Endosulfan	4.45 ± 1.38	375 ± 70	6	11
#110	2.8 ± 0.14	43 ± 11	11	16	Endosulfan sulfate	0.07 ± 0.06	26 ± 18	9	14
#118	1.08 ± 0.05	81 ± 28	13	19	Endrin	<MDL	<MDL		
#128	0.05 ± 0.003	24 ± 6	7	11	α-HCH	24.53 ± 11.68	78 ± 38	8	11
#132	0.51 ± 0.03	65 ± 77	8	15	β-HCH	3.73 ± 0.30	35 ± 7	11	16
#153	1.61 ± 0.08	101 ± 35	6	13	γ-HCH	4.34 ± 0.53	47 ± 7	7	10
#138	1.16 ± 0.06	102 ± 32	7	14	δ-HCH	0.28 ± 0.12	51 ± 11	13	18
#158	0.12 ± 0.01	10 ± 4	6	14	Heptachlor	1.13 ± 0.41	36 ± 11	12	16
#149	2.22 ± 0.11	67 ± 29	7	9	Hexachlorobenzene	42.71 ± 11.34	37 ± 7	9	13
#151	0.65 ± 0.03	17 ± 7	5	11	Heptachlor exo-epoxide	0.54 ± 0.43	52 ± 9	12	16
#156	0.05 ± 0.003	12 ± 5	7	12	ΣOCPs [pg/m^3]	198.62 ± 31.91	1.92 ± 0.21		
#169	<MDL	<MDL							
#170	0.11 ± 0.01	67 ± 33	6	10					
#171	0.05 ± 0.003	13 ± 5	5	8					
#177	0.09 ± 0.005	23 ± 13	4	9					
#180	0.28 ± 0.01	132 ± 79	5	8					
#183	0.15 ± 0.01	20 ± 9	4	11					
#187	0.29 ± 0.01	32 ± 19	5	10					
#191	0.01 ± 0.002	3 ± 1	8	12					
#194	0.01 ± 0.003	37 ± 32	7	10					
#195	0.01 ± 0.001	11 ± 8	6	9					
#201	0.03 ± 0.002	21 ± 19	4	7					
#205	0.003 ± 0.001	4 ± 2	6	9					
#206	0.01 ± 0.001	38 ± 35	6	11					
#208	0.01 ± 0.001	7 ± 5	5	9					
#209	0.01 ± 0.001	55 ± 33	4	6					
ΣPCBs [pg/m^3]	215 ± 10.96	1.9 ± 0.32							

D-score absolute values for tetra-CBs were also higher (average 24 and 19) than those of penta- to nona-CBs (up to 13, except PCB #101). Most reference mass fractions for PCBs (all remaining congeners, see Figs. 3B and 3D) were likewise adequately recovered, whereas a similar trend of increasing recovery with increasing degree of chlorination was also apparent (Fig. 3D). Less chlorinated biphenyls (e.g. PCBs #17, 18, 44 and less likely #70) of reference mass classified fractions scored relatively higher D- values (average 23–34), compared to those of higher chlorination (average 2–14).

Chlorinated pesticides, such as *trans*-chlordane, *p,p'*-DDD and *p,p'*-DDE, were also measured close to their certified values (96, 95 and 102% average recoveries, respectively) (Fig. 3D), with |D-score| values from 2 to 5. Additionally, *cis*- (90%) and oxychlordane (97%), *p,p'*-DDT (98%), *o,p'*-DDT and its metabolites (*o,p'*-DDD/E; 95–98%) exhibited equally sufficient recovery ranges, close to their reference mass fractions (Fig. 3D). The z- versus ζ-scores scatterplot for PCBs and OCPs (Fig. 3B) demonstrated an overall agreement of SRM 1649b urban dust measured concentrations with the corresponding certified and/or reference values. Most chlorinated compounds lied within, or close to the respective acceptance threshold values (Fig. 3D; blue highlighted area), except for some tri-CBs (e.g. #17, 18), oxychlordane and PCBs #177 and 205 in a limited number of replicate SRM measurements.

Application to atmospheric samples

The proposed method was separately applied to six pairs of gaseous and particulate phase samples (see also section 2.2). Each sample underwent the entire procedure of analysis and the corresponding measured concentrations (average ± 1σ) are presented

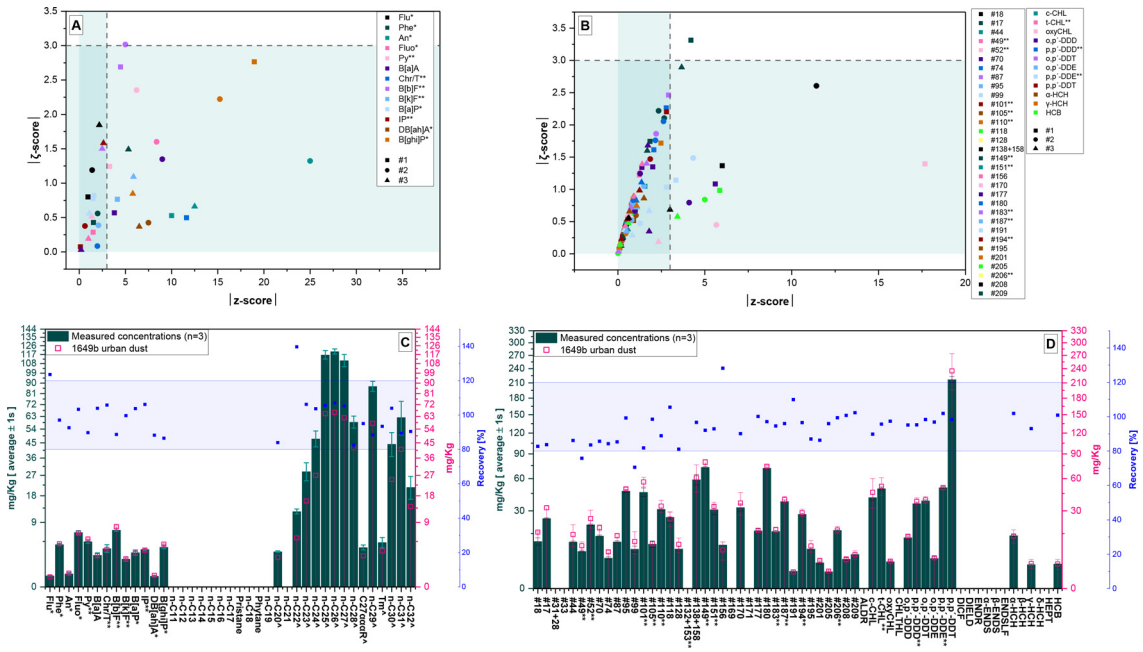

Fig. 3. Scatterplots of z- versus ζ- absolute scores for PAHs (panel A), PCBs and OCPs (panel B). Acceptance threshold values for both scores are also highlighted by light blue areas. Measured (n = 3) concentrations (average ± 1σ) of NIST's SRM 1649b (urban dust) compared to the corresponding certified, reference and information values for aliphatics and PAHs (panel C), PCBs and OCPs (panel D). The corresponding recovery percentages are also displayed by blue scatter dots. For panels A, C: *reference values; **certified values; ^information values. For panels B, D: **certified values; all remaining compounds: reference values. Compounds presented with no bars in panels C and D were not included in NIST's urban dust reference material.

in Tables 2 (for PAHs and aliphatics) and 3 (for PCBs and OCPs). Extracted ion chromatograms of characteristic homologue and/or member groups of PCBs, OCPs and PAHs are also shown in Fig. 4.

All target compounds were identified, except for endrin and PCB #169, which were both not detected in any of the collected gas and particulate phase samples (Table 3). The isomers β-, γ- and δ-HCH, *o,p'*-DDT, *o,p'*-DDE, aldrin, as well as PCBs #18, 87, 99, 206 and 208 were quantified in at least one particulate phase sample, whereas *o,p'*-DDD, *p,p'*-DDD, β-HCH and γ-HCH were correspondingly identified in at least one gas phase sample (Table 3). On the contrary, *o,p'*-DDD, *p,p'*-DDT and PCB #33 were identified in none of the particulate phase samples (Table 3).

Total atmospheric (gas and particulate phase) concentrations of *n*-alkanes, isoprenoid (pristane, phytane) and triterpenoid (*Tm*, C30$\alpha\beta$, C27$\alpha\alpha\alpha$R) hydrocarbons were on average 32.54 (± 8.70), 10.46 (± 2.43), 6.94 (± 4.95), 0.05 (± 0.02), 0.06 (± 0.02) and 0.27 (± 0.20) ng/m^3, respectively (Table 2). Long chain *n*-alkanes with $C_n > C_{25}$ were measured at higher levels in particulate phase, whereas in gas phase, *n*-alkanes with $C_n < C_{25}$ exhibited higher concentrations, due to their semivolatility [48]. A pattern of higher odd-carbon number *n*-alkane homologue distribution (C_{25}, C_{27}, C_{29}, C_{31}, C_{33}) was also observed in particulate phase, indicative of higher plant leaf wax source contributions from the surrounding environment [17]. Dominant PAH members in the gas phase were those of lower molecular weight (fluorene to chrysene/triphenylene), whereas in particulate phase, heavy PAHs (benzo[*b*]fluoranthene to benzo[*ghi*]perylene) exhibited higher concentrations (Table 2). We measured ca. three times lower total *n*-alkanes ($\Sigma n\text{-}C_n$) concentrations, compared to those reported at an urban site (average 89 ng/m^3) in Athens, Greece [48]. The corresponding concentrations of pristane, phytane, *Tm* and C30$\alpha\beta$ in the aforementioned site (2.8, 4.3, 0.05 and 0.10 ng/m^3, respectively) approached those of our study (Table 2). Unlike *n*-alkanes, we measured slightly lower total (gas and particulate phase) Σ_{13}PAH concentrations (average 20.78 ± 8.29 ng/m^3; Table 2), compared to those reported in the urban site of Athens, Greece (average Σ_{13}PAHs 17.5 ng/m^3) [48].

Relatively similar, to those of our study, total (gas and particulate phase) concentrations for the less chlorinated (PCBs #28 and 52) of the seven PCB indicators (#28, 52, 101, 118, 138, 153, and 180) were reported in the urban site of Athens, Greece (30, 25, 21, 10, 3 and 7 pg/m^3, respectively) [48]. However, in a study conducted by our group three years ago at Nicosia, Cyprus [8], comparable total (gas and particulate phase) concentrations, with those reported herein (Table 3), for all PCB indicators were measured (19, 46, 6, 1, 1, 2 and 0.6 pg/m^3). Similar observations have been obtained for most OCPs as well (Table 3). Between the aforementioned [8] and the current study, both been conducted in the same urban location, potential differences in mass distribution of PCBs and OCPs were of insignificant magnitude. Most abundant members were on average DDX (72.13 pg/m^3; sum of *o,p'*-DDD, *o,p'*-DDE, *o,p'*-DDT, *p,p'*-DDD, *p,p'*-DDE and *p,p'*-DDT), following by HCHs (54.27 pg/m^3; sum of α- β-, γ-, and δ-HCH) and HCB (43.78 pg/m^3) (Table 3). 2Heptachlors (1.22 pg/m^3; sum of heptachlor and heptachlor epoxide) and drins (2.04 pg/m^3; sum of aldrin and dieldrin) were the least abundant OCPs reported herein (Table 3).

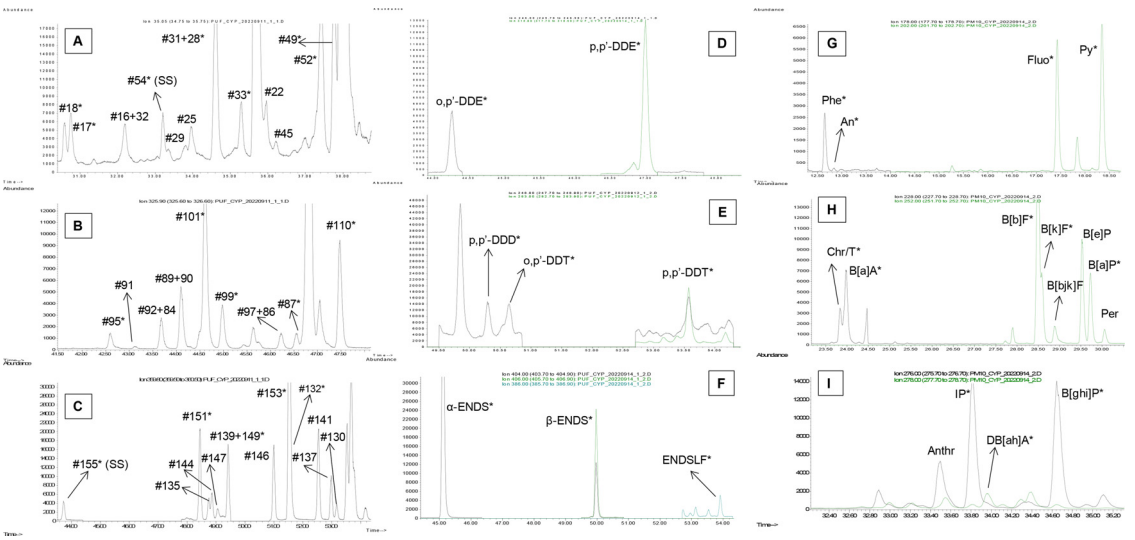

Fig. 4. Extract ion chromatograms of characteristic homologue/member groups of PCBs (panel A: tri- and tetra-CBs; panel B: penta-CBs; panel C: hexa-CBs), OCPs (panels D-F) and PAHs (panels G-I) obtained from the analysis of an atmospheric sample. Analytes included in standard solutions are annotated with an asterisk (*). SS: surrogate standard. The co-eluted PCB homologues were identified based on the study of Frame [49] and Mandalakis et al. [37].

Conclusions

A simple multi-residue analytical method has been developed for a wide variety of halogenated POPs (forty-two PCB congeners, twenty-four OCP compounds) and molecular tracers (full range of PAHs, *n*-alkanes, isoprenoid and triterpenoid hydrocarbons) in atmospheric samples, which expands from purification to chemical analysis by GC-LRMS operating in EI and ECNI mode. All target compounds were successfully recovered by an adsorption column, packed with activated silica gel, florisil and neutral alumina, in two subsequent elution fractions i) with *n*-hexane, and ii) a mixture of *n*-hexane and dichloromethane, both of low volume. To the best of our knowledge, this study is the first that evaluates the optimum mass spectrometric parameters (ion source temperature, electron energy and emission current) for PCBs and OCPs in GC-ECNI-LRMS instruments. The analysis exhibited sufficient linearity and low inter- and intra-day variability. The method was effectively validated by repeatable analyses of a certified reference material (NIST 1649b urban dust), and successfully applied to actual atmospheric (gas and particulate phase) samples. The proposed method is selective, precise, practical and provides an affordable sample preparation procedure for the vast number of research labs equipped with conventional instrumentation on a routine basis, over laborious and/or cost-consuming analytical techniques.

Declaration of Competing Interest

The authors declare that they have no known competing financial interests or personal relationships that could have appeared to influence the work reported in this paper.

CRediT authorship contribution statement

Minas Iakovides: Conceptualization, Methodology, Investigation, Resources, Formal analysis, Data curation, Validation, Visualization, Writing – original draft. **Jean Sciare:** Funding acquisition, Supervision, Writing – review & editing. **Nikos Mihalopoulos:** Funding acquisition, Supervision, Writing – review & editing.

Data availability

Data will be made available on request.

Acknowledgments

The present work received funding from the European Union's Horizon 2020 research and innovation program under grant agreement No. 856612 (EMME-CARE) and the Cyprus Government.

Supplementary materials

Supplementary material associated with this article can be found, in the online version, at doi:10.1016/j.mex.2023.102224.

References

[1] J.R. Barrett, POPs vs. Fat: persistent organic pollutant toxicity targets and is modulated by adipose tissue, Environ. Health Perspect. 121 (2013) a61-a61.
[2] K. Borgå, M.A. McKinney, H. Routti, K.J. Fernie, J. Giebichenstein, I. Hallanger, et al., The influence of global climate change on accumulation and toxicity of persistent organic pollutants and chemicals of emerging concern in Arctic food webs, Environ. Sci.: Process. Impacts 24 (2022) 1544–1576.
[3] J.K. Schuster, T. Harner, A. Eng, C. Rauert, K. Su, K.C. Hornbuckle, et al., Tracking POPs in global air from the first 10 years of the GAPS network (2005 to 2014), Environ. Sci. Technol. 55 (2021) 9479–9488.
[4] S. Sinkkonen, J. Paasivirta, Degradation half-life times of PCDDs, PCDFs and PCBs for environmental fate modeling, Chemosphere 40 (2000) 943–949.
[5] Hageman K.J., Bogdal C., Scheringer M. Chapter 11 - long-range and regional atmospheric transport of pops and implications for global cycling. In: Zeng EY, ed. Comprehensive Analytical Chemistry. 67. Elsevier, 2015, pp. 363–387.
[6] UNEP. Stockholm convention secretariat. http://chm.pops.int/. Accessed Nov. 2022.
[7] G. Abbasi, L. Li, K. Breivik, Global historical stocks and emissions of PBDEs, Environ. Sci. Technol. 53 (2019) 6330–6340.
[8] M. Iakovides, K. Oikonomou, J. Sciare, N. Mihalopoulos, Evidence of stockpile contamination for legacy polychlorinated biphenyls and organochlorine pesticides in the urban environment of Cyprus (Eastern Mediterranean): influence of meteorology on air level variability and gas/particle partitioning based on equilibrium and steady-state models, J. Hazard. Mater. 439 (2022) 129544.
[9] L. Melymuk, J. Blumenthal, O. Sáňka, A. Shu-Yin, V. Singla, K. Šebková, et al., Persistent problem: global challenges to managing PCBs, Environ. Sci. Technol. 56 (2022) 9029–9040.
[10] A.M. Taiwo, A review of environmental and health effects of organochlorine pesticide residues in Africa, Chemosphere 220 (2019) 1126–1140.
[11] L. Famiyeh, K. Chen, J. Xu, Y. Sun, Q. Guo, C. Wang, et al., A review on analysis methods, source identification, and cancer risk evaluation of atmospheric polycyclic aromatic hydrocarbons, Sci. Total Environ. 789 (2021) 147741.
[12] K.-.H. Kim, S.A. Jahan, E. Kabir, R.J.C. Brown, A review of airborne polycyclic aromatic hydrocarbons (PAHs) and their human health effects, Environ. Int. 60 (2013) 71–80.
[13] K. Sun, Y. Song, F. He, M. Jing, J. Tang, R. Liu, A review of human and animals exposure to polycyclic aromatic hydrocarbons: health risk and adverse effects, photo-induced toxicity and regulating effect of microplastics, Sci. Total Environ. 773 (2021) 145403.
[14] G. Lammel, Polycyclic aromatic compounds in the atmosphere – a review identifying research needs, Polycycl. Aromat. Compd. 35 (2015) 316–329.
[15] N.-.D. Dat, M.B. Chang, Review on characteristics of PAHs in atmosphere, anthropogenic sources and control technologies, Sci. Total Environ. 609 (2017) 682–693.
[16] W. Ye, X. Xu, M. Zhan, Q. Huang, X. Li, W. Jiao, et al., Formation behavior of PAHs during pyrolysis of waste tires, J. Hazard. Mater. 435 (2022) 128997.
[17] M. Iakovides, G. Iakovides, E.G. Stephanou, Atmospheric particle-bound polycyclic aromatic hydrocarbons, n-alkanes, hopanes, steranes and trace metals: PM2.5 source identification, individual and cumulative multi-pathway lifetime cancer risk assessment in the urban environment, Sci. Total Environ. 752 (2021) 141834.
[18] I. Tsiodra, G. Grivas, K. Tavernaraki, A. Bougiatioti, M. Apostolaki, D. Paraskevopoulou, et al., Annual exposure to polycyclic aromatic hydrocarbons in urban environments linked to wintertime wood-burning episodes, Atmos. Chem. Phys. 21 (2021) 17865–17883.
[19] G. Lammel, F.X. Meixner, B. Vrana, C.I. Efstathiou, J. Kohoutek, P. Kukučka, et al., Bidirectional air–sea exchange and accumulation of POPs (PAHs, PCBs, OCPs and PBDEs) in the nocturnal marine boundary layer, Atmos. Chem. Phys. 16 (2016) 6381–6393.
[20] M. Wietzoreck, M. Kyprianou, B.A. Musa Bandowe, S. Celik, J.N. Crowley, F. Drewnick, et al., Polycyclic aromatic hydrocarbons (PAHs) and their alkylated, nitrated and oxygenated derivatives in the atmosphere over the Mediterranean and Middle East seas, Atmos. Chem. Phys. 22 (2022) 8739–8766.
[21] J.F. Pankow, T.F. Bidleman, Interdependence of the slopes and intercepts from log-log correlations of measured gas-particle paritioning and vapor pressure—I. theory and analysis of available data, Atmos. Environ. Part A. Gen. Topics 26 (1992) 1071–1080.
[22] R.L. Falconer, T.F. Bidleman, Vapor pressures and predicted particle/gas distributions of polychlorinated biphenyl congeners as functions of temperature and ortho-chlorine substitution, Atmos. Environ. 28 (1994) 547–554.
[23] H.A. Leslie, B. van Bavel, E. Abad, J. de Boer, Towards comparable POPs data worldwide with global monitoring data and analytical capacity building in Africa, Central and Latin America, and the South Pacific, TrAC Trends Analyt. Chem. 46 (2013) 85–97.
[24] E.J. Reiner, K.J. Jobst, D. Megson, F.L. Dorman, J.-.F. Focant, Chapter 3 - analytical methodology of POPs, in: G O'Sullivan, C Sandau (Eds.), Environmental Forensics for Persistent Organic Pollutants, Elsevier, Amsterdam, 2014, pp. 59–139.
[25] I.G. Kavouras, E.G. Stephanou, Direct evidence of atmospheric secondary organic aerosol formation in forest atmosphere through heteromolecular nucleation, Environ. Sci. Technol. 36 (2002) 5083–5091.
[26] L. Melymuk, P. Bohlin, O. Sáňka, K. Pozo, J. Klánová, Current challenges in air sampling of semivolatile organic contaminants: sampling artifacts and their influence on data comparability, Environ. Sci. Technol. 48 (2014) 14077–14091.
[27] L. Melymuk, P. Bohlin-Nizzetto, R. Prokeš, P. Kukučka, J. Klánová, Sampling artifacts in active air sampling of semivolatile organic contaminants: comparing theoretical and measured artifacts and evaluating implications for monitoring networks, Environ. Pollut. 217 (2016) 97–106.
[28] A. Maceira, R.M. Marcé, F. Borrull, Analytical methods for determining organic compounds present in the particulate matter from outdoor air, TrAC Trends Analyt. Chem. 122 (2020) 115707.
[29] A.M. Muscalu, T. Górecki, Comprehensive two-dimensional gas chromatography in environmental analysis, TrAC Trends Analyt. Chem. 106 (2018) 225–245.
[30] Y. Pico, A.H. Alfarhan, D. Barcelo, How recent innovations in gas chromatography-mass spectrometry have improved pesticide residue determination: an alternative technique to be in your radar, TrAC Trends Analyt. Chem. 122 (2020) 115720.
[31] P. Sathishkumar, K. Mohan, A.R. Ganesan, M. Govarthanan, A.R.M. Yusoff, F.L. Gu, Persistence, toxicological effect and ecological issues of endosulfan – a review, J. Hazard. Mater. 416 (2021) 125779.
[32] H.-.G. Ni, H. Zeng, E.Y. Zeng, Sampling and analytical framework for routine environmental monitoring of organic pollutants, TrAC Trends Analyt. Chem. 30 (2011) 1549–1559.
[33] J. Kwan, Europe's energy crisis hits science hard, Science (New York, NY) 377 (2022) 1244–1245.
[34] B. Owens, Energy crisis squeezes science at CERN and other major facilities, Nature 610 (2022) 431–432.
[35] M. Iakovides, M. Apostolaki, E.G Stephanou, PAHs, PCBs and organochlorine pesticides in the atmosphere of Eastern Mediterranean: investigation of their occurrence, sources and gas-particle partitioning in relation to air mass transport pathways, Atmos. Environ. 244 (2021) 117931.
[36] Wells D.E. Chapter 4 current developments in the analysis of polychlorinated biphenyls (Pcbs) including planar and other toxic metabolites in environmental matrices. In: Barceló D, ed. Techniques and Instrumentation in Analytical Chemistry. 13. Elsevier, 1993, pp. 113–148.
[37] M. Mandalakis, M. Tsapakis, E.G. Stephanou, Optimization and application of high-resolution gas chromatography with ion trap tandem mass spectrometry to the determination of polychlorinated biphenyls in atmospheric aerosols, J. Chromatogr. A 925 (1–2) (2001) 183–196.
[38] C. Yang, G. Zhang, Z. Wang, Z. Yang, B. Hollebone, M. Landriault, et al., Development of a methodology for accurate quantitation of alkylated polycyclic aromatic hydrocarbons in petroleum and oil contaminated environmental samples, Analyt. Methods 6 (2014) 7760–7771.
[39] M. Otto, Chemometrics: Statistics and Computer Application in Analytical Chemistry, John Wiley & Sons, 2016.
[40] L.K. Ackerman, G.R. Wilson, S.L. Simonich, Quantitative analysis of 39 polybrominated diphenyl ethers by isotope dilution GC/low-resolution MS, Anal. Chem. 77 (2005) 1979–1987.
[41] J. Björklund, P. Tollbäck, C. Östman, Mass spectrometric characteristics of decabromodiphenyl ether and the application of isotopic dilution in the electron capture negative ionization mode for the analysis of polybrominated diphenyl ethers, J. Mass Spectrom. 38 (2003) 394–400.
[42] Jürgen Schulz H. Analysis of pharmacologically relevant compounds using GC/MSD-EI/PCI/NCI. 2002.
[43] J.A. Laramée, R.B. Cody, M.L. Deinzer, Discrete energy electron capture negative ion mass spectrometry, Encycl. Analyt. Chem. (2006).
[44] Schulz J.H. Analysis of pharmacologically relevant compounds using GC/MSD-EI/PCI/NCI. Agilent Technologies Waldbronn 2002; Compendium of Applications.
[45] E.S. Chernetsova, A.I. Revelsky, I.A. Revelsky, I.A. Mikhasenko, T.G. Sobolevsky, Determination of polychlorinated dibenzo-p-dioxins, dibenzofurans, and biphenyls by gas chromatography/mass spectrometry in the negative chemical ionization mode with different reagent gases, Mass Spectrom. Rev. 21 (2002) 373–387.

[46] Gonzalez C., Choquette S. Certificate of analysis: standard reference material 1649b, 2016.
[47] Analytical Methods Committee AN, z-Scores and other scores in chemical proficiency testing—their meanings, and some common misconceptions, Analyt. Methods 8 (2016) 5553–5555.
[48] M. Mandalakis, M. Tsapakis, A. Tsoga, E.G Stephanou, Gas–particle concentrations and distribution of aliphatic hydrocarbons, PAHs, PCBs and PCDD/Fs in the atmosphere of Athens (Greece), Atmos. Environ. 36 (2002) 4023–4035.
[49] G.M. Frame, A collaborative study of 209 PCB congeners and 6 Aroclors on 20 different HRGC columns1. Retention and coelution database, Fresenius J. Anal. Chem. 357 (1997) 701–713.